Proceedings of the 1996 IEEE/SICE/RSJ International Conference on Multisensor Fusion and Integration for Intelligent Systems

# Dead Reckoning Navigation of a Mobile Robot Using an Indirect Kalman Filter

KyuCheol Park

Automatic Control Research Center, School of Electrical Engineering Seoul National University, Seoul, 151-742, KOREA pkc@asrignc1.snu.ac.kr

Dohyoung Chung

Multimedia R&D Center Samsung Electronics CO., LTD., Suwon, 440-600, KOREA dhchung@khgw.info.samsung.co.kr

Hakyoung Chung

Department of Control and Instrumentation Engineering, Seoul National Polytechnic University, Seoul, 139-240, KOREA chy@duck.snpu.ac.kr

Jang Gyu Lee

Automatic Control Research Center, School of Electrical Engineering Seoul National University, Seoul, 151-742, KOREA jgl@asrignc1.snu.ac.kr

## Abstracts

*An encoder and a gyroscope fusion algorithm for an Autonomous Mobile Robot navigation using indirect Kalman filter scheme is proposed. Encoder based navigation algorithm is developed and, based on the navigation algorithm, a navigation error model is derived by linear perturbation. The indirect Kalman filter for fusion algorithm is realized by applying Kalman filter to the navigation error model. Furthermore the use of indirect feedback Kalman filter, which feeds back the error estimates to the main navigation algorithm is proposed for the AMR navigation. The simulation is performed and the results show that the navigation algorithm with the indirect feedback Kalman filter can successfully combine the encoder and gyroscope measurements and estimate the position and heading angle of the AMR.*

## 1. Introduction

Dead reckoning is the most popular navigation system for autonomous mobile robots(AMR) and odometer is the most simplistic implementation of dead reckoning. Odometer provides a position and an orientation of the mobile robot by using onboard encoder information. The advantages in using the encoder navigation system are that the encoders are inexpensive and can provide relatively accurate information if the encoder errors are carefully calibrated[1,2]. However, the error due to slippage, misalignment of wheels, etc. is accumulated without bounds. Therefore, other navigation techniques have been applied to reduce the effects of such encoder errors.

Inertial navigation system is a sophisticated implementation of dead reckoning, which uses inertial sensors such as gyroscopes, accelerometers to measure the angular velocity and the linear acceleration with respect to the inertial space. The angular velocity from gyroscope can be integrated to provide the heading, and the linear acceleration from accelerometers is integrated to provide the velocity for the AMR. Besides the deterministic errors contained in gyroscope and accelerometer measurements, they also have stochastic errors which call for the use of estimation and optimal filtering to correct them.

The recent development of inexpensive inertial sensors gives ways to broad applications of inertial sensors to the AMR navigation[3 – 7]. Barshan and Durrant-Whyte proposed an inertial sensor error model and the use of *Extended Kalman filter* algorithm based on the error model [3,4]. The proposed *EKF* uses gyroscope and accelerometer measurements to estimate the position and heading angle of an AMR. Komoriya and Oyama also proposed the *EKF* algorithm which uses gyroscope measurements to estimate the heading angle of an AMR[6]. These *EKF* algorithms correspond to the *direct Kalman filter* scheme for conventional inertial navigation system[8]. Hence they also embody the drawbacks of the *direct Kalman filter* scheme, one of which is that if the *EKF* happens to fail, such as the divergence of error covariance, the entire navigation system can not provide the position and heading angle of the AMR. The *direct Kalman filter* scheme also requires rapid computations of Kalman filter at least the twice the rate of AMR dynamics. However the use of the *indirect Kalman filter* scheme avoid such drawbacks[10]. Furthermore by combining the encoder measurements and the inertial sensor measurements using the *indirect Kalman filter*, it is possible to be mutually benefited from each other. By augmenting the encoder error states and inertial sensor error states, designed Kalman filter enables the estimation and correction of both sensor error states.

Our research aims at developing a reliable position and heading angle estimator for the AMR navigation system which combines an encoder and a gyroscope using the *indirect Kalman filter* algorithm. The previous *EKF* estimates the position and heading angle but the *indirect Kalman filter* estimates the position error, the heading angle error, velocity error, encoder and gyroscope errors, instead. These estimated errors are fed back into the AMR navigation system to compensate the navigation errors and to keep the linearity of the error characteristics, hence achieving the *indirect feedback Kalman filter* methodology. As the difference between the encoder and the gyroscope is taken as the measurement for the indirect Kalman filter, the errors in the encoder and the gyroscope are mutually compensated. In this way, the linear characteristics of the error dynamics are maintained and Kalman filter performance is enhanced. Moreover, the navigation system can use the unfiltered position and heading angle of AMR when the filter fails since the indirect feedback Kalman filter does not *directly* estimate the position and heading angle of AMR.

## 2. AMR navigation system

The AMR navigation system consists of the navigation system equations and the navigation error equations. The navigation system equations produce the position and heading angle of the AMR. The navigation error equations are used in the indirect feedback Kalman filter.

### 2.1 Position and Heading angle Computation

Consider two coordinates shown in figure 1. The OXYZ coordinate is the navigation frame and the oxyz is the body frame of AMR and its origin is located at the center of the AMR. The AMR position and heading angle are computed by the differential encoder. In the followings, the variables with superscript *b* and *n* represent the body frame and the navigation frame respectively. The subscript *en* represents the encoder. The subscript *el* and *er* represent the left-hand side encoder and right-hand side encoder respectively.

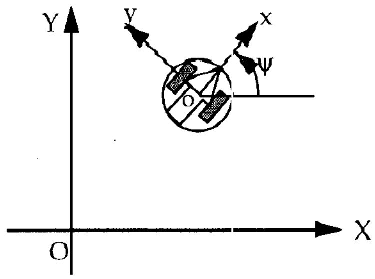


Fig. 1. Body and navigation frame of the AMR

$$\begin{bmatrix} \dot{X}^n_{en} \\ \dot{Y}^n_{en} \end{bmatrix} = \begin{bmatrix} \cos\psi & -\sin\psi \\ \sin\psi & \cos\psi \end{bmatrix} \mathbf{v}^b_{en}, \quad \mathbf{v}^b_{en} \equiv \frac{1}{2}\begin{bmatrix} v^b_{er} + v^b_{el} \\ 0 \end{bmatrix} \tag{1}$$

$$\dot{\psi}^n_{en} = \frac{v^b_{er} - v^b_{el}}{D}$$

where

| | |
|---|---|
| $X, Y$ | AMR position in the navigation frame. |
| $\psi$ | The heading angle of the AMR or The angle between the body frame and the navigation frame |
| $v^b_{er}, v^b_{el}$ | The right and left encoder velocity measured at the body frame |
| $D$ | The distance between the left and right wheel of the AMR |

### 2.2 Position and heading angle error equation.

The following error equations are derived using the linear perturbation method. It is well known that encoder error sources fit into one of two categories : systematic errors and non-systematic errors [4,5].

Systematic Errors
1. Unequal wheel diameters which can be defined as encoder velocity scale factor errors
2. Difference between the actual wheel-base and the nominal wheel-base
3. Misalignment of wheels
4. Finite encoder resolution
5. Finite encoder sampling rate

Non - Systematic Errors
1. Travel over uneven floors
2. Travel over unexpected objects on the floor
3. Wheel slippage

In this work, we are mainly concerned to reduce the systematic errors. The wheel diameter error and the wheel base error are the dominant systematic errors of the encoder system. $\delta D$ represents the wheel-base error.

The right and left encoder velocity represented in the body frame is

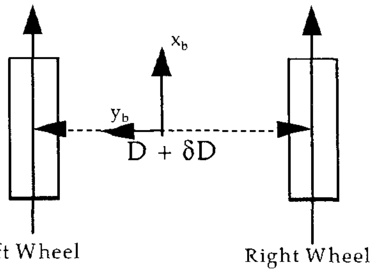


Fig. 2. Encoder Wheel Diagram

$$\hat{\mathbf{v}}^{\mathbf{b}}_{\mathbf{er}} = \begin{bmatrix} \hat{v}^b_{er,x} \\ \hat{v}^b_{er,y} \end{bmatrix} = \begin{bmatrix} v^e_{er} + s_1 v^e_{er} \\ 0 \end{bmatrix}, \quad \hat{\mathbf{v}}^{\mathbf{b}}_{\mathbf{el}} = \begin{bmatrix} \hat{v}^b_{el,x} \\ \hat{v}^b_{el,y} \end{bmatrix} = \begin{bmatrix} v^e_{el} + s_2 v^e_{el} \\ 0 \end{bmatrix} \tag{2}$$

where $s_1$ and $s_2$ are the scale factor errors of the right encoder and the left encoder, respectively. Hence the x and y velocity in the body frame is

$$\hat{\mathbf{v}}^{\mathbf{b}}_{\mathbf{en}} = \frac{1}{2}\begin{bmatrix} v^e_{er} + s_1 v^e_{er} \\ 0 \end{bmatrix} + \frac{1}{2}\begin{bmatrix} v^e_{el} + s_2 v^e_{el} \\ 0 \end{bmatrix}. \tag{3}$$

The angular velocity in the body frame is

$$\hat{\psi}^b_{en} = \hat{\omega}^b_{en} = \frac{\hat{v}^b_{er} - \hat{v}^b_{el}}{D + \delta D}.$$

The angular velocity error equation can be derived by subtracting the true angular velocity from the calculated angular velocity.

$$\begin{aligned} \delta\psi^b_{en} = \delta\omega^b_{en} &= \frac{\hat{v}^b_{er,x} - \hat{v}^b_{el,x}}{D + \delta D} - \frac{v^b_{er} - v^b_{el}}{D} \\ &\cong \frac{1}{D}\left(s_1 v^e_{er} - s_2 v^e_{el}\right) - \frac{1}{D^2}\left(v^e_{er} - v^e_{el}\right)\delta D \end{aligned} \tag{4}$$

where we assume that $D^2 >> \delta D D$.

Similarly, the x and y velocity error equation in the body frame is

$$\begin{bmatrix} \delta\dot{x}^b_{en} \\ \delta\dot{y}^b_{en} \end{bmatrix} = \delta\mathbf{v}^{\mathbf{b}}_{\mathbf{en}} = \hat{\mathbf{v}}^{\mathbf{b}}_{\mathbf{en}} - \mathbf{v}^{\mathbf{b}}_{\mathbf{en}} = \frac{1}{2}\begin{bmatrix} s_1 v^e_{er} + s_2 v^e_{el} \\ 0 \end{bmatrix}, \tag{5}$$

and the X and Y velocity error equation in the navigation frame is

$$\begin{aligned} \begin{bmatrix} \delta\dot{X}^n_{en} \\ \delta\dot{Y}^n_{en} \end{bmatrix} &= \delta\mathbf{V}^n_{\mathbf{en}} = \hat{\mathbf{V}}^n_{en} - \mathbf{V}^n_{en} \\ &= \begin{bmatrix} -V^n_{en,Y} \\ V^n_{en,X} \end{bmatrix}\delta\psi + \frac{1}{2}\begin{bmatrix} \cos\psi & -\sin\psi \\ \sin\psi & \cos\psi \end{bmatrix}\begin{bmatrix} s_1 v^e_{er} + s_2 v^e_{el} \\ 0 \end{bmatrix} \end{aligned} \tag{6}$$

where we assume that $\cos\delta\psi \cong 1$, $\sin\delta\psi \cong \delta\psi$ and $\delta\psi\delta v^b_{en} \cong 0$.

### 2.3 Encoder Error Model

The scale factor error and the wheel base error can be regarded as random constants because these errors have very slow time-varying characteristics.

$$\dot{s}_1 = 0, \dot{s}_2 = 0, \delta\dot{D} = 0 \tag{7}$$

### 2.4 Gyroscope error model[8,9]

The dominant gyroscope random errors are the random bias and the scale factor error. Generally, the gyroscope output signal is not zero even though there is no input and the effect of the earth rotation is neglected; there is some offset caused by manufacturing imperfections, called gyro bias. The bias error can be modeled as random constant or random bias. The random constant is described by the differential equation

$$dx(t)/dt = 0 \tag{8}$$

The scale factor relates the output of the gyroscope to the corresponding gyroscope rotation angle about its input axis. The scale factor error can be modeled as the first order Markov process.

$$\dot{\psi}_{gyro} = (S + B_s)\Omega + B_{rb}(1 - e^{-\frac{t}{T}}) + v(t) \tag{9}$$

where $\Omega$ is the true angular rate, $S$ is the gyroscope scale factor (unit : $^\circ$/sec/volt), $B_{rb}$ is random bias, $B_s$ is the gyroscope scale factor error and $v(t)$ is white noise. Using the perturbation methods, we can derive the following gyroscope error equations.

$$\begin{aligned} \delta\dot{\psi} &= \delta B_s\Omega + \delta B_{rb}(1 - e^{-\frac{t}{T}}) + v \\ \delta\dot{B}_s &= -\frac{1}{T_s}\delta B_s + w \\ \delta\dot{B}_{rb} &= 0 \end{aligned} \tag{10}$$

where $v$ and $w$ are the white noise.

## 3. Indirect Feedback Kalman filter

Due to the stochastic nature of the errors in the inertial sensors, Kalman filter is often used in modern inertial navigation system. There are two formulations in applying Kalman filter to the navigation system for the error compensation ; *direct* versus *indirect* filtering[8]. As the name indicates, in the *direct* formulation, the states such as the position and velocity are among the state variables in the filter, and the measurement are inertial sensors outputs and external sensors outputs. In the *indirect* formulation, the errors in the position and heading angle are among the estimated variables, and each measurement to the filter is the difference between inertial sensors and external sensors.

The direct filter formulation for AMR navigation, as depicted in figure 3, was proposed and used by the Barshan *et al* and Komoriya *et al*[3,4,6]. In this direct structure, the Kalman filter is *in* the navigation loop. The benefit of this structure is that the optimal time-varying gains can provide substantial improvements in performance over classical approaches, which use fixed gain updating. However, there are several very serious drawbacks in this implementation.

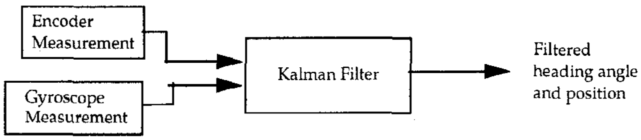


Fig. 3. AMR navigation with Direct Kalman Filter

First, being in the navigation loop, the filter would have to maintain explicit, accurate awareness of AMR's linear and angular motion as well as attempt to suppress noisy and erroneous sensor data. Due to the accuracy and the continuous demand of AMR's position and heading data, the direct Kalman filter approach should be performed at least twice the frequency of AMR dynamics. Furthermore, the direct Kalman filter requires much computational burden since the amount of computation required for Kalman filter is generally proportional to the cubic square of the number of the state variables. Seconds, when the filter happens to fail, the entire AMR navigation system fails. The AMR navigation system cannot operate without the filter. Furthermore, previous approaches use the encoder and the gyroscope exclusively. Therefore, the filter does not correct the encoder and the gyroscope error mutually but only attempts to suppress their errors based on the independent error models.

These described drawbacks can be solved by the indirect Kalman filter. Because the filter is *out* of the navigation loop as shown in figure 4, the filter can be run at the relatively slow rate and the unaltered encoder navigation system information would still be available even if the filter fails.

In the indirect Kalman filter, the AMR's position, velocity and heading angle error become the candidates for state variables.

Once the error states are estimated by the designed indirect Kalman filter, the error estimates can be used to compensate the AMR's position and heading angle. The measurement for the Kalman filter can be provided by the difference between inertial sensors outputs and encoder outputs. Depending on the treatment of the error estimates, there are two types of indirect Kalman filter implementation, *feedforward* and *feedback*. In the *feedforward* configuration the encoder navigation system operates as though there were no aiding, and its outputs are compensated using the error estimates.

However, the encoder navigation system is free to drift with unbounded errors due to the encoder sensor characteristics and the divergence of the error state due to the error model inadequacy can occur. Thus, the *indirect feedback* Kalman filter configuration is suggested for AMR navigation system(Fig. 4). In the *indirect feedback* Kalman filter configuration, the Kalman filter estimates the errors in the AMR navigation outputs, then they are fed back into the encoder navigation system. Thus, the navigation sensors errors are kept small by the Kalman filter and the adequacy of the linear error model is maintained.

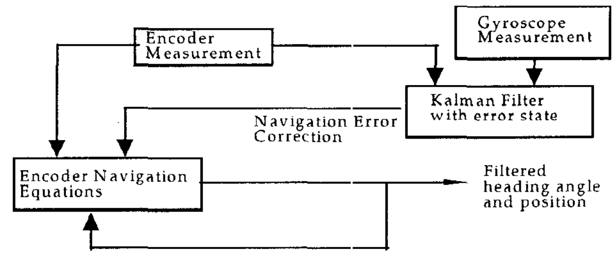


Fig. 4. AMR navigation with indirect feedback Kalman Filter

This indirect Kalman filter structure can reduce the computational burden and can also reduce the effects of inertial sensor drift and error accumulation. Furthermore, the random characteristics of the gyroscope are considered in gyroscope error modeling.

For the indirect Kalman filter design, the system matrix $\dot{x} = Ax + Q$ is

$$\begin{bmatrix} \delta\dot{X} \\ \delta\dot{Y} \\ \delta\dot{\psi} \\ \dot{s}_1 \\ \dot{s}_2 \\ \delta\dot{D} \\ \delta\dot{\psi}_g \\ \delta\dot{B}_s \\ \delta\dot{B}_{rb} \end{bmatrix} = \begin{bmatrix} 0 & 0 & -V^n_{en,Y} & \frac{1}{2}\cos\psi v^e_{er} & \frac{1}{2}\cos\psi v^e_{el} & 0 & 0 & 0 & 0 \\ 0 & 0 & V^n_{en,X} & \frac{1}{2}\sin\psi v^e_{er} & \frac{1}{2}\sin\psi v^e_{el} & 0 & 0 & 0 & 0 \\ 0 & 0 & 0 & \frac{1}{D}v^e_{er} & -\frac{1}{D}v^e_{el} & \frac{1}{D^2}(v^e_{el} - v^e_{er}) & 0 & 0 & 0 \\ 0 & 0 & 0 & 0 & 0 & 0 & 0 & 0 & 0 \\ 0 & 0 & 0 & 0 & 0 & 0 & 0 & 0 & 0 \\ 0 & 0 & 0 & 0 & 0 & 0 & 0 & 0 & 0 \\ 0 & 0 & 0 & 0 & 0 & 0 & 0 & \Omega & 1-e^{-\frac{t}{T}} \\ 0 & 0 & 0 & 0 & 0 & 0 & 0 & 0 & -\frac{1}{T_s} \\ 0 & 0 & 0 & 0 & 0 & 0 & 0 & 0 & 0 \end{bmatrix} \begin{bmatrix} \delta X \\ \delta Y \\ \delta\psi \\ s_1 \\ s_2 \\ \delta D \\ \delta\psi_g \\ \delta B_s \\ \delta B_{rb} \end{bmatrix} + Q \tag{11}$$

where $Q$ is the process noise.
and the measurement equation $Z = Hx + R$ is

$$Z = \hat{\omega}^b_{encoder} - \hat{\omega}^b_{gyro} = \delta\psi_e - \delta\psi_g$$

$$= \begin{bmatrix} \frac{1}{D}v^e_{er} & -\frac{1}{D}v^e_{el} & \frac{1}{D^2}(v^e_{er} - v^e_{el}) & -\Omega & -1 + e^{-\frac{t}{T}} \end{bmatrix} \begin{bmatrix} s_1 \\ s_2 \\ \delta D \\ \delta B_s \\ \delta B_{rb} \end{bmatrix} + R \tag{12}$$

where $R$ is the measurement noise.

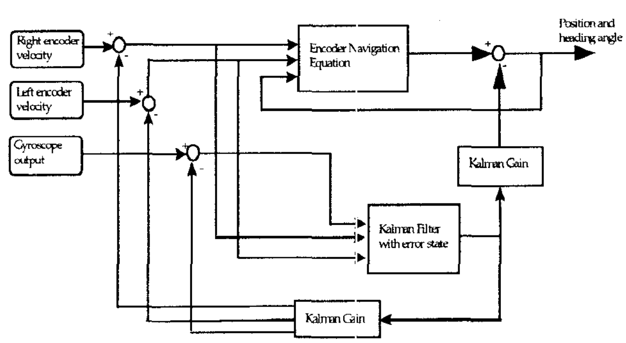


Fig. 5. AMR navigation system block diagram

As the difference between the encoder angular velocity and the gyroscope is used for the filter measurement, the indirect feedback Kalman filter can compensate the encoder error and the gyroscope error mutually through the indirect feedback Kalman filter.

## 4. Simulation Results

The specifications of the gyroscope and the encoder are shown in Table 1. Each value in the Table 1 represents the RMS 1 sigma value. The *EKF* and indirect feedback Kalman filter results are compared for four different trajectories. The *EKF* estimates heading angle using the gyroscope and calculates the position and heading angle of AMR.

The trajectories are a 5 meter straight line, a 5x5 meter square path, '8' type path and a stairs-type path. The AMR navigates about 30 minutes in each trajectory and Monte-Carlo simulations are performed. For the error analysis, the standard deviation of the difference value between the true value of the x, y position and heading angle and the estimated value of the x, y position and heading angle are calculated. To measure the preciseness of the estimated position and heading angle, Circular Error Probability (CEP)[10] is introduced. The CEP is the radius of a circle that encloses 50% of the probability hit. Therefore the smaller the CEP, the smaller the errors and hence, the more accurate system. The approximated CEP can be calculated by the equation(13)

$$CEP = 0.589(\sigma_x + \sigma_y) \quad (13)$$

where $\sigma_x$ and $\sigma_y$ are the X and Y axis standard deviation respectively.

Table 1. Error Characteristics

| Encoder Error Characteristics | | Gyroscope Error Characteristics | |
|---|---|---|---|
| Scale Factor Error | 0.5 % | Random bias | 18 °/hour (1 $\sigma$ value) |
| Wheel-base Error | 0.005 m (1 $\sigma$ value) | Scale Factor Error | 1 % |

In every simulation, the AMR moves with the linear velocity 0.25 m/sec and 30 °/sec angular velocity. The coordinate (x, y, °) denotes the x, y position in meter and heading angle in degree. In the followings, the filter denotes the indirect feedback Kalman filter and EKF denotes the extended Kalman filter.

### 4.1 5 meter straight line

The AMR moves 5 meters along the $x$ axis. When the AMR reaches the (5, 0, 0°), then the AMR stops and turns 180° counter-clockwise. The AMR comes back to the origin along the $x$ axis and turns 180° clockwise. The AMR repeats this trajectory 19 times which takes about 30 minutes. As shown in figure 7, the CEP with filter is smaller than the CEP with *EKF*. When the AMR runs the straight line, the encoder can compensate the gyroscope drift errors as the

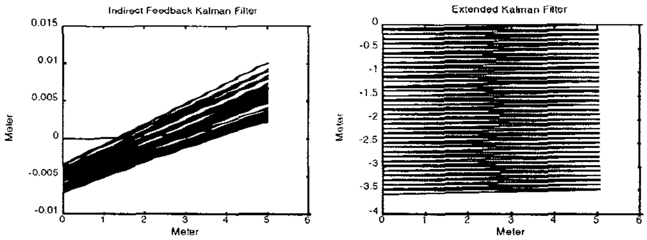


Fig. 6. AMR trajectories of the 5 meter straight moving back and forward
Final position : Filter (0.0053, -0.0036, 0.1527°), EKF(0.0464, -3.5895, 0.0013°)

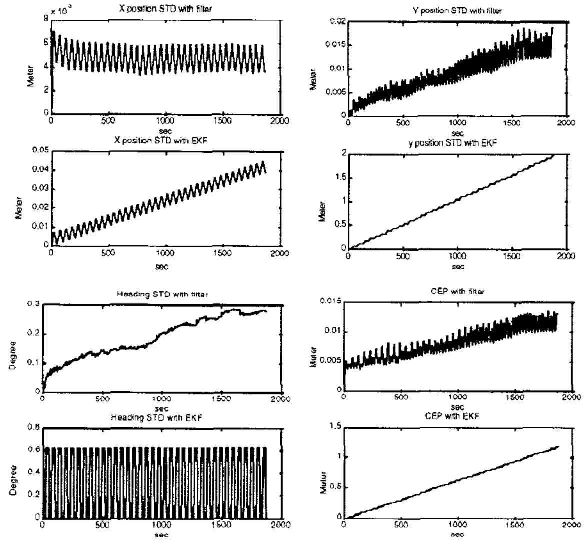


Fig. 7. The standard deviation of the position and heading angle and the CEP

angular velocity from the encoder is close to zero. However, the *EKF* does not utilize the encoder advantage but only tries to reject the gyroscope error using the gyroscope error model.

### 4.2 5x5 meter square path

Figure 8 shows the 5x5 meter square path. The AMR movements are (0, 0, 0°) → (5, 0, 90°) → (5, 5, 180°) → (0, 5, 270°) → (0, 0, 0°). The AMR repeats the trajectory 19 times. As the AMR runs the square path in counter-clockwise, the small heading angle error may generate the large position error. While the AMR runs the straight line, the heading angle from the gyroscope output is corrupted by the gyroscope drift error. Accordingly the AMR deviates from the straight line. Moreover, the accumulated heading angle error can cause the *EKF* misleading while AMR rotates. However, the indirect feedback Kalman filter compensates the encoder error using the gyroscope especially during the AMR rotation and corrects the gyroscope error using the encoder while the AMR running the straight line.

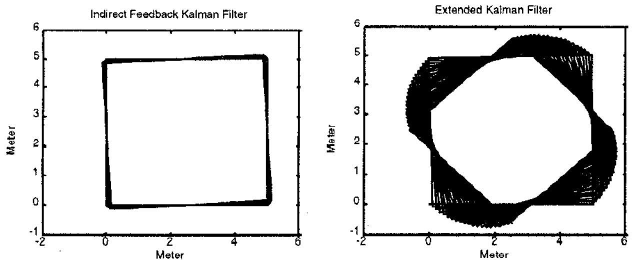


Fig. 8. AMR trajectories and CEP's of the 5×5 meter square path
Final position : Filter (0.1658, -0.1448, 363.4923°), EKF (2.5185, -0.6341, 135.5626°)

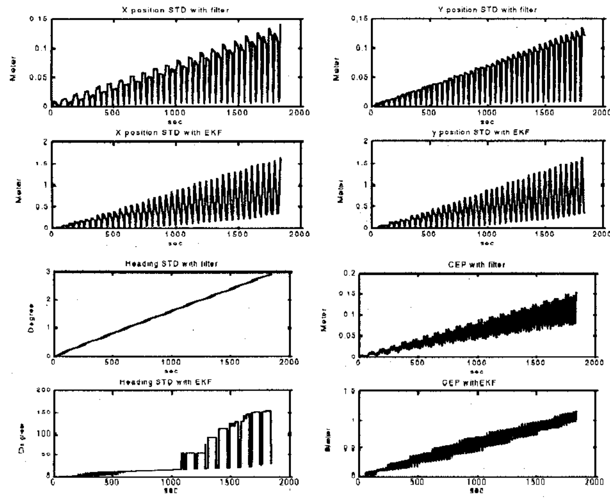

Fig. 9. The standard deviation of the position and heading angle and the CEP

### 4.3 '8' type path

The AMR movements are (0, 0, 0°) → (5, 0, 90°) → (5, 5, 0°) → (10, 5, -90°) → (10, 0, 180) → (5, 0, 90) → (5, 5, 180°) → (0, 5, -90°) → (0, 0, 0°). The AMR repeats the trajectory 9 times. As mentioned in square path simulation section, the heading angle error causes the position error. However, the AMR rotates clockwise and counter-clockwise, the CEP is smaller than that of the square path. This result comes from that the encoder scale factor error and wheel-base error are canceled by rotating clockwise and counter-clockwise in turn.

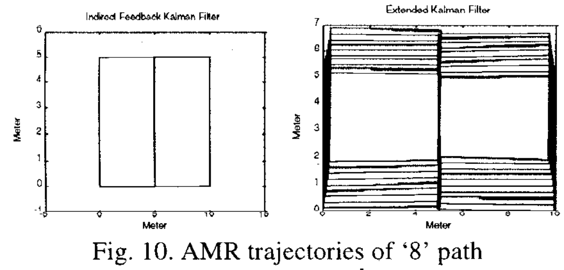


Fig. 10. AMR trajectories of '8' path
Final position : Filter (0.0015, -0.0272, 0.2712°), EKF (0.2822, 2.1194, 3.5944°)

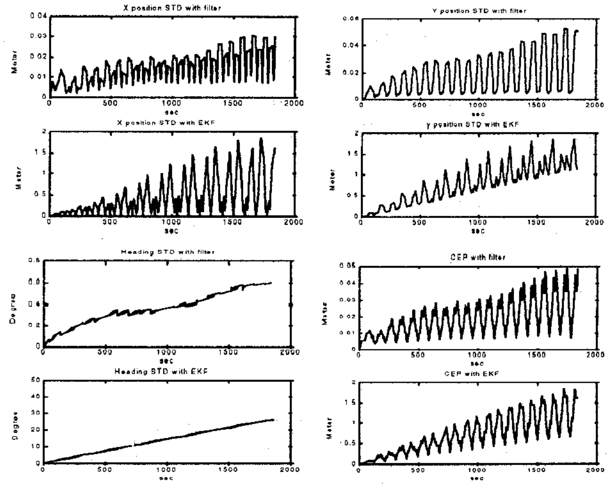

Fig. 11. The standard deviation of the position and heading angle and the CEP

### 4.4 Stairs type path

The AMR movements are (0, 0, 0°) → (2.5, 0, 90°) → (2.5, 2.5, 0°) → (5, 2.5, 90°) → (5, 5, 0°) → (7.5, 5, 180°) → (5, 5, 270°) → (5, 2.5, 180°) → (2.5, 2.5, 270°) → (2.5, 0, 180°) → (0, 0, 0°). The AMR repeats the trajectory 12 times. The CEP is also smaller than the that of the square path. Furthermore, the CEP is smaller than that of '8' path as the AMR turns alternatively clockwise and counter-clockwise in stairs type path.

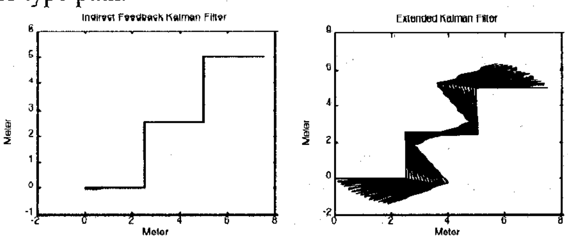


Fig. 12. AMR trajectories of stairs type path
Final position : Filter (-0.0004, -0.0102, 0.5337°), EKF (1.8913, -1.4259, 31.0171°)

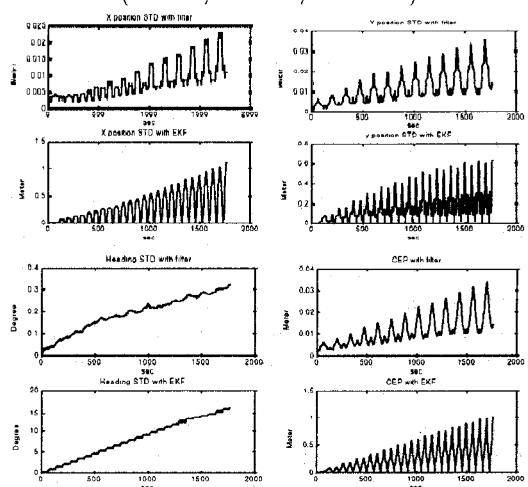

Fig. 13. The standard deviation of the position and heading angle and the CEP

Every simulation results show that the indirect feedback Kalman filter estimates position and heading angle more precisely than *EKF* does. The accumulated gyroscope heading error produces the position error in *EKF* filtering. As *EKF* does not fuse the encoder and the gyroscope, the position and heading error grows more rapidly than that of the indirect feedback Kalman filter. However, the indirect feedback Kalman filter effectively combines the encoder and gyroscope to estimate the position and heading angle of AMR.

## 5. Discussions

The AMR navigation algorithm which combines an encoder and a gyroscope to provide the position and heading angle of the AMR is suggested. The proposed AMR navigation system basically depends on the encoder and calibrates the encoder errors using the gyroscope. Since the gyroscope output need not be integrated, the navigation system can be free from the gyroscope drift error accumulation. Instead of using the direct Kalman filter, the indirect feedback Kalman filter is adopted for the AMR navigation since it can relatively well prevent the sensor error from the divergence and can keep the linear error dynamics model. Furthermore, the indirect feedback Kalman filter can compensate the encoder errors and the gyroscope errors mutually. The proposed estimation and compensation algorithm using the indirect feedback Kalman filter can reduce the computational burden because it can be run at a slower rate than previously proposed algorithms. The simulation results show that using indirect feedback Kalman filter scheme the AMR navigation system with the encoder and gyroscope can give precise position and heading angle information about 30 minutes without any help from the other external positioning aids.

## References


[1] Borentein, J. and Feng, L. 1995a, "Correction of Systematic Dead-reckoning Errors in Mobile Robots." *1995 International Conference on Intelligent Robots and Systems(IROS '95)*. Pittsburgh, PA, Aug. 5-9, pp.569-574.

[2] Borentein, J. and Feng, L. 1995b, "UMBmark : A Method for Measuring, Comparing, and Correcting Dead-reckoning Errors in Mobile Robots." Technical report UM-MEAM-94-22, University of Michigan

[3] Barshan, B. and Durrant-Whyte, H. F., 1994, "Orientation Estimate for Mobile Robots Using Gyroscopic Information." 1994 International Conference on Intelligent Robots and Systems(IROS '94). Munich, Germany, Sept. 12-16, pp. 2243-2248.

[4] Barshan, B. and Durrant-Whyte, H. F., 1995, "Inertial Navigation Systems Mobile Robots." *IEEE Transaction on Robotics and Automation*, Vol. 11, No. 3, June, pp. 328-342.

[5] Borentein, J. and Feng, L. 1995c, "Where am I ? Sensors and Methods for Autonomous Mobile Robot Positioning - 1995 Edition"

[6] Komoriya, K. and Oyama, E., 1994, "Position Estimation of a Mobile Robot Using Optical Fiber Gyroscope(OFG)." *1994 International Conference on Intelligent Robots and Systems(IROS '94)*. Munich, Germany, Sept. 12-16, pp. 143-149.

[7] Vaganay, J., Aldon, M. J., and Fourinier, A., 1993, "Mobile Robot Attitude Estimation by Fusion of Inertial Data." *Proceedings of IEEE International Conference on Robotics and Automation*, Atlanta, GA, May 2-7, pp. 3243-3248.

[8] Maybeck, P. S. "Stochastic models, estimation, and Control Volume 1." Academic Press. 1979

[9] Lawrence, A., "Modern Inertial Technology - Navigation, Guidance, and Control." Springer-Verlang. 1993

[10] Siouris G. M. " Aerospace Avionics Systems - A Modern Synthesis." Academic Press 1993.

[11] Betke, M. and Gurvits, L., 1994, "Mobile Robot Localization Using Landmarks." *1994 International Conference on Intelligent Robots and Systems(IROS '94)*. Munich, Germany, Sept. 12-16, pp. 135-142.

[12] Kleeman, L., 1992, "Optimal Estimation of Position and Heading for Mobile Robot Using Ultrasonic Beacons and Dead-reckoning." *Proceedings of IEEE International Conference on Robotics and Automation*, Nice, France, May 12-14, pp. 2582-2587.